

Phase Structure of Systems with Infinite Numbers of Absorbing States

M. A. Muñoz,^{1,2} G. Grinstein,¹ and R. Dickman^{3,4}

Received September 30, 1997

Critical properties of systems exhibiting phase transitions into phases with infinite numbers of absorbing states are studied. We analyze a non-Markovian Langevin equation recently proposed to describe the critical behavior of such systems, and also introduce and study a non-Markovian discrete model, which is argued to present the same critical features. On the basis of mean-field analysis, Monte Carlo simulations, and theoretical arguments, we conclude that the phenomenology of the non-Markovian models closely parallels that of systems with many absorbing states in one and two dimensions. The “bulk” or “static” critical properties of these systems fall in the directed percolation (DP) universality class. By contrast, the critical properties associated with the spread of an initially localized seed exhibit a more complex behavior: Depending on parameter values they can, both in one and two dimensions, fall either in the dynamical percolation or DP universality class, or else exhibit apparently nonuniversal exponents. In contrast to previous results, however, the nonuniversal exponents in 2D are found to satisfy a scaling law which implies that a particular linear combination of them is universal and assumes DP values. These results demonstrate the efficacy of the non-Markovian approach for understanding systems with many absorbing states, which are difficult to analyze in their original microscopic formulation.

KEY WORDS: Nonequilibrium phase transitions; absorbing states.

I. INTRODUCTION

Absorbing configurations are microscopic states in which a system can be trapped, and from which it can never escape. Often the phase diagram of

¹ IBM T. J. Watson Research Center, Yorktown Heights, New York 10598.

² Dipartimento di Fisica, Università di Roma “La Sapienza,” I-00185 Rome, Italy.

³ Department of Physics and Astronomy, Herbert H. Lehman College, City University of New York, Bronx, New York 10468.

⁴ Departamento de Física, Universidade Federal de Santa Catarina, Campus Universitário-Trindade, CEP 88040-900, Florianópolis-SC, Brazil.

a system exhibiting absorbing states contains a nonequilibrium critical point (or surface of critical points) separating an *absorbing phase*, where the only steady states are absorbing states, from an *active phase* in which a non-trivial steady-state dynamics occurs.

Phase transitions into absorbing states occur in many different models in physics, chemistry, biology, and economics, and so have received much attention in the last years. Among others, the family of systems with absorbing states includes the following models and systems: directed percolation (DP),⁽¹⁻³⁾ surface reaction models,^(4, 5) branching and annihilating random walks,⁽⁶⁾ the contact process,^(7, 2, 3) models of catalytic reactions,^(8, 9) systems with multiplicative noise,⁽¹⁰⁻¹³⁾ damage spreading transitions,⁽¹⁴⁾ models of epidemics and of forest fires,⁽¹⁵⁻¹⁷⁾ models of transport in porous media and growing surfaces pinned by impurities,^(18, 19) and even models of self-organized criticality.⁽²⁰⁾

Usually, in studies of systems with absorbing states, two different types of analysis are performed:

- Studies in which the initial condition is homogeneously random are typically used to determine standard bulk quantities of interest such as the averaged order parameter, M , the correlation length, ξ , or correlation time τ , as a function of the distance, Δ , to the critical point. The critical exponents β , ν_x and ν_t , defined by

$$M(\Delta) \sim \Delta^\beta \quad (1)$$

$$\xi(\Delta) \sim \Delta^{-\nu_x} \quad (2)$$

$$\tau(\Delta) \sim \Delta^{-\nu_t} \quad (3)$$

respectively, are determined in this manner. The approach of different quantities towards the steady state, for example, $M(t) \sim t^{-\theta}$ at criticality, can also be analyzed in this way.

- Studies of the spreading of a localized initial seed in an otherwise absorbing configuration⁽²¹⁾ yield further insight into the physics of absorbing states. A spreading critical point separates an active region, in which the initial seed spreads indefinitely, from an absorbing region, in which it dies out with unit probability as $t \rightarrow \infty$.⁵ The quantities usually computed in this type of study are: the total number of active sites, $N(t)$, averaged over all runs (including those which have reached the absorbing state); the mean-square distance, $R^2(t)$, of active sites from the original seed in surviving trials; and the survival probability, $P(t)$, i.e., the probability that the

⁵ We shall see that the critical point for spreading often, but not always, coincides with the bulk critical point.

system has not reached the absorbing state at a given time t .⁶ At the critical point these quantities scale for large t like:

$$N(t) \sim t^\eta \quad (4)$$

$$R^2(t) \sim t^z \quad (5)$$

$$P(t) \sim t^{-\delta} \quad (6)$$

which respectively define the exponents η , z , and δ .

From now on we refer to the quantities or critical exponents calculated with these two approaches as *bulk* and *spreading* properties respectively. In DP and related models, the bulk and spreading critical points coincide, and the two sets of exponents are connected through scaling relations such as $\beta = \delta \nu_t$.

An ambitious task in this area is that of assigning all the different phase transitions into absorbing states to appropriate universality classes. The main breakthrough in this direction is due to Janssen⁽²²⁾ and Grassberger,⁽²³⁾ who conjectured some time ago that all models exhibiting a continuous transition into a unique absorbing state with no extra symmetry or conservation law belong in the same universality class, namely that of DP. (This universality class is described by Reggeon field theory (RFT), a model first introduced in the realm of particle physics^(24, 25)). This conjecture is supported by a large number of both numerical and analytical studies.^(26, 27)

Other universality classes, different from DP, have been identified subsequently. They describe phase transitions with essential physical differences with respect to DP. Some of them are:

- Certain models of epidemics and forest fires,^(15, 16) have been found to be represented by a history-dependent field theory, in which the dynamics at the critical point generates percolation clusters. This is the so-called *dynamical percolation* universality class, and is a time-dependent generalization of standard percolation.⁽¹⁵⁾

- In particle systems in which evolution occurs only at the interfaces separating occupied from empty (absorbing) regions, compact clusters are generated, rather than the fractal clusters generated by more generic rules, such as DP, that allow evolution within the bulk occupied regions. These models belong to the *compact directed percolation* (CDP) or *voter model*

⁶ Note that $N(t)$ is computed by averaging over all the runs, while $R^2(t)$ is calculated by averaging only over the runs that have not reached an absorbing state at time t . The average number of active sites in the surviving runs, $N_s(t)$, satisfies $N(t) = N_s(t) P(t)$, and therefore scales asymptotically like $t^{\eta+\delta}$.

universality class.⁽²⁸⁾ A field theory for such systems can be found in refs. 29 and 30.

- There are systems with absorbing states in which the total number of particles is conserved (locally) modulo two, i.e., the parity of the particle number is conserved. It is well established by now that this extra conservation law puts such models in a new universality class, different from DP.^(31, 6) A field theory describing this class has recently been proposed.^(6, 32)

- A new universality class characterized by noise different from that of the previously described classes has recently been elucidated. It is called the *multiplicative noise* (MN) universality class, and describes absorbing-state systems wherein the dominant source of noise is external. (See refs. 11, 12, 10, and 13 and references therein for more details.)

In this paper, we study a related but somewhat more complex problem, namely, the critical behavior of systems with an *infinite number of absorbing states* (INAS, hereafter). Such systems arise in many of the same contexts (notably catalysis,^(33, 4, 5, 34) and epidemiology^(15, 16)), that give rise to models with unique absorbing states. In the typical situation of interest, the number of distinct absorbing configurations grows exponentially with system size. We focus here on the pair contact process (PCP),^(35, 36) a prototypical simple model of this type, which has been studied quite extensively through simulations, and found to exhibit complex critical behavior that is only partially understood. We will not consider models such as the threshold transfer process (TTP),^(37, 36) which also have INAS, but whose behavior is somewhat simpler⁽³⁶⁾.

The PCP is a particle system or cellular automaton, similar in spirit to the well known contact process (CP),⁽³⁸⁾ but with the evolution controlled by nearest neighbor (NN) pairs of particles. The model is described as follows: Particles are distributed on a regular d -dimensional lattice, each site being either singly occupied or empty. An isolated particle, that is, one with no occupied nearest neighbor, cannot change its state. On the other hand, a NN particle pair can either annihilate, producing two new empty sites (with probability p), or, with probability $1 - p$, generate a new particle on a randomly chosen, empty, neighboring site, if there is one. The details of the implementation of this basic idea in a specific algorithm do not affect the qualitative features or critical behavior of the model. It is clear that any configuration of isolated particles is absorbing under these general rules. The number of such configurations obviously grows exponentially with system size. The PCP has been shown numerically to undergo a continuous transition from an active to an absorbing phase⁽³⁵⁾ as p increases. The phenomenology of this transition is quite complex: While bulk critical properties seem to belong in the DP universality class, the spreading

properties show evidence of nonuniversal behavior. In the next section we summarize these numerical results, and the fairly complete understanding of the bulk properties that has recently been developed. In Section III we study the spreading problem in mean-field theory. In Section IV we introduce and study numerically a new microscopic model, argued to belong in the same universality class as systems with INAS. Comparing the results for this model with those of Section III, we propose an explanation for some of the nonuniversality in spreading properties observed in two-dimensional (2D) models with INAS. We also observe that the nonuniversal exponents of our new model in 2D satisfy a scaling law postulated earlier, that has been previously observed to hold in 1D but not in 2D. In consequence, a particular linear combination of the nonuniversal exponents assumes a universal, DP value. Section V summarizes our results and conclusions.

II. SYSTEMS WITH AN INFINITE NUMBER OF ABSORBING STATES: SUMMARY OF PREVIOUS RESULTS

A. Numerical Results

1. One Dimension ($d=1$). After some initial controversy, it now seems clear from Monte Carlo simulations that all bulk critical exponents measured thus far in models with infinite numbers of absorbing states^(35, 4, 5, 34) assume DP values. Critical spreading, however, presents a more complex and puzzling picture. At the critical point for spreading (which coincides with the bulk critical point), the statistics of surviving trials (i.e., runs that have not reached an absorbing configuration at a given time), coincide with those of the surviving trials in DP, implying that both z and the combination $\eta + \delta$ are universal, with DP values, in $d=1$.⁽³⁵⁾ Surprisingly, however, the exponents associated with quantities averaged over *all* the runs, such as η and δ individually, are found to be non-universal, varying with the type of absorbing state invaded by the initial seed, i.e., on the initial condition. (For the 1D PCP model, e.g., δ has been found to assume values between roughly 0.09 and 0.25, while η varies between 0.38 to 0.21 as the initial conditions are modified.⁽³⁵⁾ For DP, recall, $\delta \approx 0.16$, and $\eta \approx 0.31$.) Only for the so-called “natural-initial-state” initial condition are DP exponents recovered. As detailed in ref. 35, the natural initial state consists of absorbing configurations generated by the model itself, at the critical point, starting from a homogeneous configuration.

For any type of initial condition, a generalized hyperscaling relation postulated for these systems,^(37, 35, 39) namely,

$$2(\delta + \tilde{\delta}) + 2\eta = dz \tag{7}$$

is observed to hold. Here $\tilde{\theta}$ is a new universal exponent, defined through the asymptotic time dependence of the mean density of particles in the occupied region, $n(t) \sim t^{-\tilde{\theta}}$, resulting from an initial seed, averaged only over surviving trials at criticality. In DP it can be shown^(21, 39) that $\tilde{\theta} = \delta$ and therefore the scaling relation reads $4\delta + 2\eta = dz$. Note that $\tilde{\theta} = \theta$ always.

So far there is no satisfactory theoretical understanding of all these facts, in particular of the non-universality.

2. Two Dimensions ($d=2$). As in $d=1$, all the bulk critical exponents are found to assume DP values (see ref. 40 and references therein). The situation regarding spreading exponents seems, however, even more complicated than in $d=1$;⁽⁴⁰⁾ all of them seem to be non-universal: δ can change by more than one order of magnitude with changing initial conditions, and neither z nor $\eta + \delta$ is constant, as they were in $d=1$. Furthermore, the scaling relation derived for systems with INAS, Eq. (7),^(37, 39, 40) seems to be violated. The critical point for the spreading of a seed is found to depend on the initial condition, and does not coincide, in general, with the critical point for bulk properties. This shift in the critical point is believed to be the origin of the violation of the scaling law. No satisfactory explanation of this complex situation has yet been proposed. (See, however, the Note Added in Proof at the end of this paper.)

B. Analytical Results

The first analytical steps in understanding the puzzling physics described above were presented in a recent paper.⁽³⁶⁾ The approach consists in describing the prototypical PCP model with two mesoscopic, coarse-grained fields, $n_1(\mathbf{x}, t)$ and $n_2(\mathbf{x}, t)$, which represent the density of isolated particles and NN pairs respectively. These fields evolve according to the following set of coupled Langevin equations:

$$\begin{aligned} \frac{\partial n_1(\mathbf{x}, t)}{\partial t} &= [r_1 + c_1 \nabla_{\mathbf{x}}^2 - u_1 n_2(\mathbf{x}, t) - w_1 n_1(\mathbf{x}, t)] n_2(\mathbf{x}, t) + n_2^{1/2} \eta_1(\mathbf{x}, t) \\ \frac{\partial n_2(\mathbf{x}, t)}{\partial t} &= [r_2 + c_2 \nabla_{\mathbf{x}}^2 - u_2 n_2(\mathbf{x}, t) - w_2 n_1(\mathbf{x}, t)] n_2(\mathbf{x}, t) + n_2^{1/2} \eta_2(\mathbf{x}, t) \end{aligned} \quad (8)$$

where the c_i , r_i , u_i , and w_i are all constants, assumed to have the appropriate signs required to keep the fields n_1 and n_2 bounded from above, and η_1 and η_2 are Gaussian white noise variables, whose only non-vanishing correlations are

$$\langle \eta_i(\vec{x}, t) \eta_j(\vec{x}', t') \rangle = D_{ij} \delta(\vec{x} - \vec{x}') \delta(t - t'), \quad (9)$$

for $i, j = 1, 2$, where the D_{ij} are noise strengths. Other higher order terms could be introduced in (8), but they can be shown to be irrelevant in the renormalization group (RG) sense.⁽³⁶⁾

As discussed in ref. 36, this set of equations can be simplified by dropping the c_1, u_1 , and noise terms in the n_1 equation, and then solving that equation for n_1 in terms of n_2 . Since the dropped terms are generated by RG iteration of the simplified equations, their omission should not change the critical properties of the system. Substituting in the n_2 equation, one obtains

$$\begin{aligned} \frac{\partial n_2}{\partial t} = & c_2 \nabla^2 n_2 + (r_2 - w_2 r_1 / w_1) n_2 - u_2 n_2^2 \\ & + w_2 (r_1 / w_1 - n_1(\vec{x}, 0)) n_2 e^{-w_1 \int_0^t n_2(\vec{x}, s) ds} + n_2^{1/2} \eta_2 \end{aligned} \quad (10)$$

where $n_1(\vec{x}, 0)$ is the initial condition of the n_1 field.

The “natural density”⁽³⁵⁾ n_1 then corresponds to the uniform density, $n_1(t=0)$, for which the coefficient of the exponential term vanishes, i.e., $n_1(t=0) = r_1 / w_1$.⁷ The equation then reduces to precisely the Langevin representation of DP. This constitutes a simple explanation of the occurrence of DP exponent values in the numerics for this special value of the initial condition.

Let us now simplify the problem by considering only uniform initial conditions, $n_1(\vec{x}, 0) = n_1$.⁸ For notational economy, we also drop the subscripts “2,” and set $r \equiv (r_2 - w_2 r_1 / w_1)$, $c_2 = 1$, and $\alpha \equiv w_2 (r_1 / w_1 - n_1)$ in Eq. (10), to obtain

$$\frac{\partial n}{\partial t} = \nabla^2 n + rn - un^2 + \alpha n e^{-w_1 \int_0^t n(\vec{x}, s) ds} + n^{1/2} \eta \quad (11)$$

which is the non-Markovian Langevin equation proposed to describe systems with INAS.

This equation is analyzed in refs. 36 and 42, with the RG. The conclusion is that for homogeneous initial conditions, the exponential term is always irrelevant, and DP-like behavior obtains, in agreement with the numerical results for $d=1$ and $d=2$. However, no prediction is made in ref. 36 for the critical spreading exponents, and in particular, no explanation for the observed non-universality has been proposed so far.

⁷This is strictly true only in mean field approximation. When the noise is considered the coefficients have to be renormalized.

⁸Straightforward application of the replica method indicates that the randomness should not do more than renormalize the coefficient of the n^2 term in Eq. (10). See, e.g., ref. 41.

III. MEAN FIELD ANALYSIS

As a first attempt to shed light on the non-universal critical spreading problem in systems with INAS, we present in this section an analysis of the Langevin Eq. (11), using a mean-field approximation wherein spatial fluctuations and the noise term are disregarded. First we discuss the case of homogeneous initial conditions, and afterwards the spreading of a seed. In both cases the effect of the non-Markovian term is analyzed, and the results compared with those of the $\alpha = 0$ case, which corresponds to the noiseless DP problem.

A. The Homogeneous Case

In the absence of noise and spatial dependence, Eq. (11) becomes

$$\frac{\partial n}{\partial t} = rn - un^2 + \alpha n e^{-w_1 \int_0^t n(s) ds} \quad (12)$$

where $n(\vec{x}, t) = n(t)$ is taken to be independent of \vec{x} . We assume that at the critical point the density $n(t)$ decays in time as a power law, $n(t) \sim t^{-\theta}$, where θ is an exponent to be determined. In the simple case $\alpha = 0$, the critical point is located at $r = 0$, whereupon Eq. (12) yields $\theta = 1$.

For the more complex case, $\alpha \neq 0$, let us first suppose that the exponent θ is smaller than 1. Then the term proportional to α would go to zero exponentially rapidly as t goes to ∞ , meaning that the non-linear term, $-un^2$, would dominate the right-hand side of Eq. (12). But this term scales like $t^{-2\theta}$, implying $\theta = 1$, in contradiction of our supposition. Next, suppose that $\theta > 1$, so that $\int_0^t ds n(s)$ approaches a constant as t goes to infinity. Writing $\exp[-w_1 \int_0^t n(s) ds] = \exp[-w_1 \int_0^\infty n(s) ds] \times \exp[w_1 \int_t^\infty n(s) ds]$, and noting that $\int_t^\infty n(s) ds \sim t^{1-\theta}$ is small for large t , we can expand the exponential term $\exp(w_1 \int_t^\infty n(s) ds)$ in powers of its argument. It follows straightforwardly that the critical point is located at $r_c = -\alpha \exp[-w_1 \int_0^\infty n(s) ds]$, and the dominant nonlinear term on the right hand side of (12) at the critical point is $\alpha w_1 n \int_t^\infty n(s) ds$. If $\alpha > 0$ this term is positive, and n grows continuously in time, contradicting our supposition. The only remaining possibility for $\alpha > 0$ is therefore $\theta = 1$. Inserting $n(t) \sim Ct^{-1}$ in (12) and performing the time integral, one sees that the exponential term behaves like t^{-Cw_1} . If $Cw_1 > 1$, the quadratic nonlinearity dominates, giving $C = 1/u$. On the other hand, if $Cw_1 < 1$, then the term proportional to α dominates, implying $Cw_1 = 1$, which is a contradiction. One concludes that for $u > w_1$, $C = 1/w_1$. In summary, then, for $\alpha > 0$, the critical point occurs at $r = 0$, where⁽⁴²⁾ $n(t) \sim C/t$, with $C = \max(1/u, 1/w_1)$.

Next consider the case $\alpha < 0$. Here the term obtained by expanding $\exp(w_1 \int_t^\infty n(s) ds)$ in power series is negative, and no contradiction with the supposition $\theta > 1$ is found. Equating the right and left hand sides of (12) produces the result $\theta = 2$.⁽⁴²⁾ It is important to note that in this case the critical value of r_c , given by $r_c = -\alpha \exp[-w_1 \int_0^\infty n(s) ds]$, depends not just on the parameters α , u , and w_1 , but on the initial value, $n(t=0)$, of n . Note too that in the active phase, i.e., when $r > r_c$, the exponential term always vanishes exponentially fast with t , and the stationarity condition implies $rn - un^2 = 0$, or $n = r/u$, in steady state. Since $r_c > 0$ when $\alpha < 0$, the mean-field phase transition in this case has some first-order character, in that there is a discontinuous jump in the value of $\langle n \rangle$ right at the critical point. Thus the critical point combines the characteristics of conventional first- and second-order transitions in this case.

Summing up, for $\alpha \geq 0$, $\theta = 1$ and the critical point is located at $r = 0$, while for $\alpha < 0$, $\theta = 2$, and the transition occurs at a value of $r > 0$ that depends on the initial conditions, and has both continuous and discontinuous characteristics. We have checked all of these results numerically, by direct integration of Eq. (12).

B. Localized Initial Seed

We now study the spreading of a localized initial seed in the mean-field approximation defined by neglecting the noise in Eq. (12). Obviously in this case the spatial dependence of $n(\vec{x}, t)$ has to be taken into account to make the approximation meaningful. The equation to be analyzed is:

$$\frac{\partial n}{\partial t} = \nabla^2 n + rn - un^2 + \alpha n e^{-w_1 \int_0^t n(\vec{x}, s) ds} \quad (13)$$

with a localized initial condition such that $n(\vec{x}, 0) \neq 0$ in a small neighborhood of $\vec{x} = \vec{0}$, and $n(\vec{x}, 0) = 0$ elsewhere. We now determine the spreading exponents δ , z , and η in this approximation.

Note that the probability of reaching the absorbing state, $n(\vec{x}, t) = 0$, is strictly zero in (13), which is a completely deterministic equation. This implies that $\delta = 0$ in the mean-field approximation.

Naive power counting in (13) shows that $t \sim x^2$, and consequently that $z = 1$. As fluctuations are not considered in mean field, that is the final result in this approximation.

The other exponent, η , is less trivial to derive, and can change depending on the parameter values, as we now show.

1. $\alpha = 0$. We start by considering the case $\alpha = 0$.

Behavior at Criticality. A localized initial seed tends to spread out and invade new regions of space, due to the diffusion term in (13). Far behind the propagating front, the Laplacian term is negligible, and the local density at every point evolves asymptotically as if from a homogeneous initial condition: n converges exponentially fast to the saturation value, r/u , if $r > 0$, or decays to 0 exponentially if $r < 0$. At $r = 0$, marginal spreading occurs, and the density in the invaded region well behind the advancing front decays to zero like $1/t$. We conclude that the critical point for spreading is located at $r = 0$, coinciding with the “bulk” critical point (see Fig. 1a). Writing the scaling Ansatz $n(\vec{x}, t) \sim f(x^2/t)/t$, where the scaling function $f(y) \rightarrow \text{constant}$ as $y \rightarrow 0$, and is exponentially small for large y , one concludes that the total number of active sites, $N(t) \equiv \int d^d x n(\vec{x}, t)$, behaves like $t^{d/2-1}$ asymptotically. That is, $\eta = -1/2$ in $d = 1$, $\eta = 0$ in $d = 2$, and $\eta = 1/2$ in $d = 3$. We have verified the 1D result numerically. Observe, however, that for dimensions larger than $d = 2$ this scaling result cannot be correct: Right at the critical point, the space integral of the equation of motion gives $\dot{N}(t) = \int d^d x \dot{n} = -u \int d^d x n^2$. Therefore $N(t)$ decreases in time, a result in obvious contradiction with η being positive for $d > 2$.

The point is that for $d > 2$, the nonlinear term un^2 is an “irrelevant” variable. To understand this, consider the diffusion equation that results from setting $u = 0$. The solution of this equation takes the scaling form $n(\vec{x}, t) \sim \tilde{f}(x^2/t)/t^{d/2}$, where \tilde{f} is a scaling function, the power $d/2$ being fixed by the requirement that $\int d^d x n(\vec{x}, t)$ be constant in time. Restoring the nonlinear term and substituting this scaling form into the equation, one sees at once that for $d > 2$ the n^2 term decays like t^{-d} at large t , i.e., more rapidly than do the derivative terms, which fall off like $t^{-(d/2+1)}$. Thus for $d > 2$ the scaling form for the diffusion equation constitutes a consistent asymptotic solution of the full equation. For $d < 2$, by contrast, the n^2 term is “relevant,” i.e., dominates at large t , demonstrating the inadequacy of the naive scaling form above. In this case, our earlier scaling form, $f(x^2/t)/t$, based on the assumption that the nonlinearity dominates the decay, is appropriate. For $d = 2$, the nonlinearity is “marginal,” and the two scaling forms coincide, both giving $\eta = 0$.

For $d > 2$, one can compute the next leading correction to n , by writing $n \sim At^{-d/2} + Bt^{-\theta_1}$ for constants A and B . Matching the large- t dependences of the left and right sides of the equation to leading and next-to-leading orders yields $\theta_1 = d - 1$. Integrating over \vec{x} then gives $N(t) \sim \tilde{A} + \tilde{B}t^{-d/2+1} + \dots$, for some constants \tilde{A} and \tilde{B} . We conclude that for $d > 2$ the exponent η sticks at its $d = 2$ value, viz., $\eta = 0$.⁹

⁹ This is consistent with the fact that η , the anomalous dimension, has to be zero at the critical dimension of RFT, $d = 4$.^(25, 39)

Supercritical Behavior. Above the critical point, $r > 0$, an initial seed spreads out rapidly due to the presence of the non-vanishing linear term in the equation of motion, and the density converges to the saturation value r/u . Since at every time step new regions are invaded, and the density in those regions grows towards the saturation value, the integral of n over all space grows linearly in time. In Fig. 1b we show the result of the numerical integration of the equation of motion in 1D: A kink propagates to the right, leaving behind a constant density. The name *Fisher waves* has been used in the literature to describe such kinks.

Subcritical Behavior. Below the critical point the initial seed dies out exponentially, and does not propagate beyond a small region around the origin. In Fig. 1c the decay observed numerically in such a case is shown.

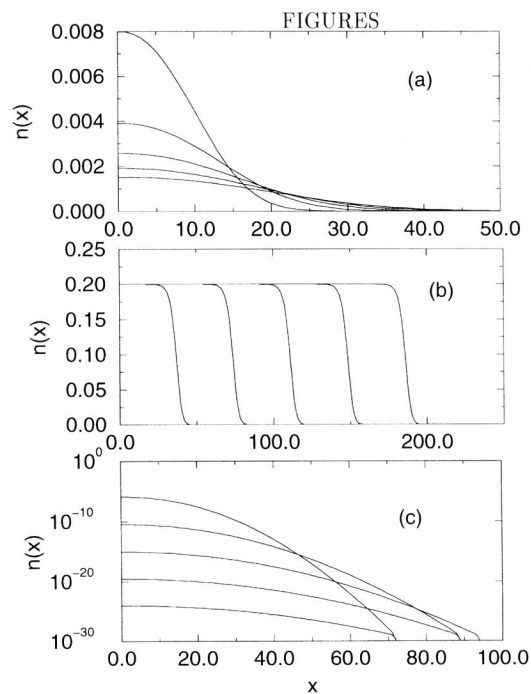


Fig. 1. Propagation of a seed in the case $\alpha = 0$, at (a) the critical point ($r = 0$); (b) above the critical point ($r = 1$); and (c) below the critical point ($r = -0.5$). Note that the scale in (c) is semi-logarithmic. The different curves correspond to $t = 200, 400, 600, 800$ and 1000 ; $u = 5$ and $w_1 = 5$ in all cases. Note that only $x > 0$ is represented.

2. $\alpha > 0$. As in the $\alpha = 0$ case, the Laplacian makes the initial seed or “bump” spread out. In this case, however, the sum $rn + \alpha n \exp(-w_1 \times \int_0^t n(s) ds)$ produces an effective linear term whose coefficient decreases monotonically with t as $\int_0^t n(s) ds$ grows, and hence is *smaller* in the central region behind the outwardly propagating front than at and ahead of the front. Thus, at and below criticality, the density decreases in the central region at a faster rate than at the borders. In other words, as the bump moves outward, its center decays rapidly, producing an expanding shell or wave of relatively high density, and leaving a relatively low-density central core in its wake.

Critical Behavior. In Fig. 2a we show the result of numerical integration in 1D at criticality, starting from seed initial conditions. The original bump splits into two pieces (only the rightmost represented in the figure),

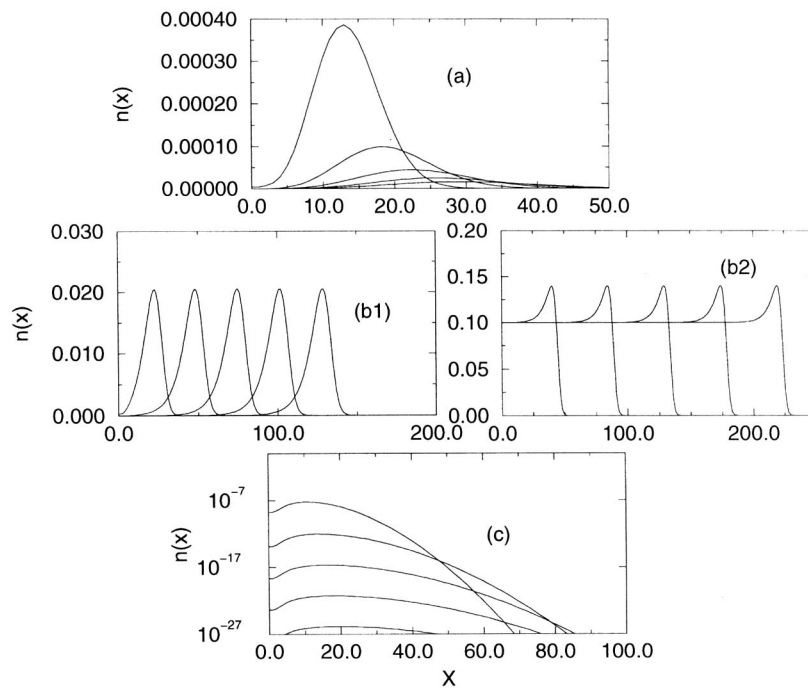


Fig. 2. Propagation of a seed in the case of $\alpha = 1$, at (a) the critical point, $r = -\alpha = -1$; (b1) above the critical point with $r = -0.5$; (b2) above the critical point, with $r = 0.5$; and (c) below the critical point. Note that the scale in (c) is semi-logarithmic. The different curves correspond to $t = 200, 400, 600, 800$ and 1000 ; $\mu = 5$ and $w_1 = 5$, and the abscissa label is x in all cases. Note that only $x > 0$ is represented.

which propagate to the right and left, the total area decreasing in time, in a manner that can be understood as follows: As the bumps propagate outward, their maximum height decreases, as shown in Fig. 2a. Concomitantly, the integral $\int_0^\infty n(\vec{x}, s) ds$ decreases with increasing distance x from the origin. It follows that for large enough x the exponential in the nonlocal term, $\alpha \exp[-w_1 \int_0^t n(\vec{x}, s) ds]$ can be expanded in powers of its argument, i.e., as $\approx \alpha - w_1 \alpha \int_0^t n(\vec{x}, s) ds$. The spreading critical point is located where the coefficient of the effective linear term vanishes, i.e., at $r_c = -\alpha$. This means that behind the bump, the effective coefficient, $r_c + \alpha e^{-w_1 \int_0^t n(s) ds}$ of the linear term is negative, implying that the asymptotic decay of the density is exponential in time. Thus virtually all of the density is contained in the bump, which spreads diffusively in time, acquiring a width L of order $t^{1/2}$, and hence a total area of $t^{d/2}$, at time t .

At criticality, we can integrate Eq. (13) over space, keeping only the dominant term on the right hand side, to obtain $\partial_t N(t) \approx -\int d\vec{x} n(\vec{x}, t) \cdot \int ds n(\vec{x}, s)$. Since $N(t) \sim t^\eta$, the value of $n(\vec{x}, t)$ averaged over the lattice (i.e., over the area, $L \sim t^{d/2}$, of the bump), scales like $t^{\eta-d/2}$. This implies that $\eta - 1 = 2(\eta - d/2) + 1 + d/2$, and consequently $\eta = -3/2$ in $d=1$. This result is reproduced in the numerical calculation: the area under the curves in Fig. 2a decays for large times like $t^{-3/2}$.

Shifting into a reference frame that moves with the maximum of the bump, we can then write the scaling Ansatz $n(\vec{y}, t) \sim t^{-\tilde{\theta}} F(y^2/t)$, where the scaling function $F(v)$ approaches a constant as $v \rightarrow 0$, while F decays exponentially fast for large v . Here y measures distances from the bump maximum. Integrating over y in d dimensions then yields $\tilde{\theta} = d/2 - \eta$, or $\tilde{\theta} = 2$ in 1D.

Supercritical Behavior. Depending on the value of r , the system exhibits two different types of behavior:

(i) $0 > r > r_c = -\alpha$. In this case the coefficient of the effective linear term, $r_{eff}(\vec{x}, t) = r + \alpha \exp(-w_1 \int_0^t n(\vec{x}, s) ds)$, is positive for points x just ahead of the outwardly moving bump or wave, where n is very small, and is negative behind the bump, where $\int_0^t n(\vec{x}, s) ds$ is larger. As the wave approaches a given point \vec{x} , $n(\vec{x}, t)$ therefore begins to grow rapidly, continuing to do so until $\int_0^t n(\vec{x}, s) ds$ has increased roughly to the point where $r_{eff}(\vec{x}, t)$ changes sign, i.e., to the point where the wave's maximum passes through \vec{x} . For subsequent times, $r_{eff}(\vec{x}, t)$ is negative, whereupon $n(\vec{x}, t)$ decays exponentially to zero. Thus the width of the bump does not spread diffusively, as it does at criticality. Rather, the bump achieves a constant width as it propagates outward. Its maximum height can also be argued to achieve a constant value: If the peak height increased with time, then $\int_0^t n(\vec{x}, s) ds$ would grow more quickly, limiting further growth of n ; while

if the peak height decreased, then $\int_0^t n(\bar{x}, s) ds$ would grow more slowly, thereby keeping r_{eff} positive longer, and producing further growth in n . Thus we are led to a picture of a well-defined wave, unchanging in shape, propagating forever outward. Our numerical solutions of the 1D equation for this case confirm this expectation (Fig. 2(b1)). Since virtually all the weight of the $n(x)$ vs x curve in this figure lies under the bump, we conclude that $N(t)$ achieves a constant value for large t : $N(t) \rightarrow N(r, \alpha)$.

The mass of the bump increases with r for fixed α as $N(r) \sim (r - r_c)^{3/2}$, and the maximum height of the bump, $m(r)$, obeys $m(r) \sim (r - r_c)^2$. These results can be easily derived from scaling: Since $N(t) \sim t^\eta$ at criticality, $N(t, r) \sim t^\eta G((r - r_c)t)$ follows from simple power counting. But $N(t) \rightarrow \text{constant}$ for $r > r_c$ and large t , so the scaling function $G(y)$ must behave like $y^{-\eta}$ for large y , whereupon $N(r) \sim (r - r_c)^{-\eta}$, i.e., $N(r) \sim (r - r_c)^{3/2}$ in 1D. Writing $N(r) = m(r) w(r)$, where $w(r)$ is the bump width, and noting that $w(r)$ scales as length, i.e., as $w(r) \sim (r - r_c)^{-1/2}$ we have $m(r) \sim (r - r_c)^{3/2+1/2} = (r - r_c)^2$ in 1D. We have verified all these 1D results numerically.

(ii) $r > 0$. The effective coefficient of the linear term in invaded regions is positive, so $n(\bar{x}, t)$ grows until it is saturated by the nonlinear term un^2 . In this way, the initial seed propagates outward, leaving behind a homogeneously occupied cluster with density $n = r/u$ (Fig. 2(b2)).

Subcritical Behavior. In this case the initial bump dies out exponentially. Fig. 2(c) shows that in 1D the maximum of the bump moves a little bit away from zero, bifurcating into two bumps which disappear rapidly.

Phase Diagram for $\alpha > 0$. At the mean-field level, the critical point for spreading, $r_c = -\alpha$, is located at a value of r smaller than the critical value, $r = 0$, separating the active and absorbing phases in the bulk. Consequently, the phase diagram is as shown in Fig. 3. In the region $0 > r > -\alpha$, which lies inside the bulk absorbing phase, an initially localized seed propagates outward indefinitely (marginally at $r = -\alpha$). This behavior is markedly different from that of DP, where infinite spreading in the absorbing phase is not possible.

It is interesting to observe that all the bulk, mean-field critical properties at $r = 0$ can be derived from

$$\dot{n} = rn + \nabla^2 n - un^2 \quad (14)$$

with $r = 0$, i.e., from the noiseless version of RFT. On the other hand, the mean-field spreading critical properties at $r = -\alpha$ can be derived from

$$\dot{n} = (r + \alpha)n + \nabla^2 n - w_1 \alpha n \int_0^t n(s) ds \quad (15)$$

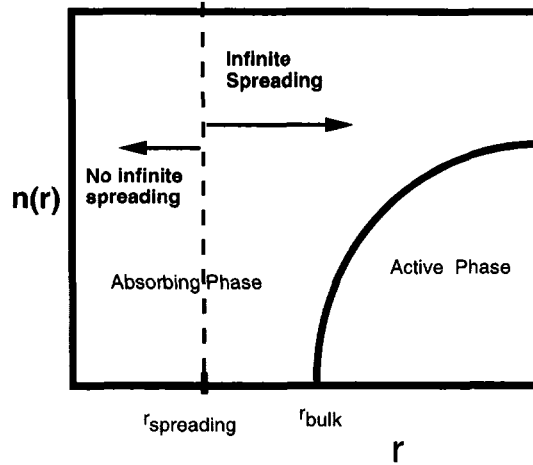


Fig. 3. Phase diagram for $\alpha = 1$: $r_{\text{spreading}} = -\alpha$; $r_{\text{bulk}} = 0$.

with $r = -\alpha$, i.e., from the noiseless version of the equation for dynamical percolation.⁽¹⁷⁾ (Note that the dynamical percolation model does not have a bulk active phase. The critical point is defined as the value of r separating the region in which an initial perturbation propagates indefinitely, from that in which it disappears.) Of course in order to reproduce the complete, mean-field phase structure (see Fig. 3), one must treat the complete Eq. (13), including the exponential term.

3. $\alpha < 0$. For $\alpha < 0$ there are again two competing effects in (13): As explained above, the Laplacian term produces the spreading of a localized seed. The term $r_{\text{eff}} = r + \alpha e^{-w_1 \int_0^z n(s) ds}$ generates a slower decay near the origin than elsewhere. That is, the decay is fastest at the border of the initial bump, where the integral in the exponential term, and hence r_{eff} , are *smallest*, thereby inhibiting spreading. This last effect is the opposite of the one observed for $\alpha > 0$, and limits the ability of the Laplacian term to produce the invasion of new regions. Moreover, the initial localized distribution is not expected to split in this case.

Critical Behavior. At any point \vec{x} , the effective coefficient of the linear term is asymptotically given by: $r + \alpha \exp[-w_1 \int_0^z ds n(\vec{x}, s)]$. Since $\alpha < 0$, the spreading critical point is expected to occur at a value $r = r_c$ satisfying $r_c + \alpha e^{-w_1 \int_0^z n(\vec{x}=0, s) ds} = 0$, so that $|\alpha| > r_c > 0$. (Note that, as in the bulk, the precise value of r_c depends not just on the parameters α , u , and w_1 , but on the initial condition $n(\vec{x}, t = 0)$.) It follows that the coefficient of the effective linear term at criticality in (13) is *negative* at the

leading edge of the bump, where the exponential term can be well approximated by α . As indicated above, no spreading therefore occurs in this case, only a small transient in which the bump spreads slightly, owing to the large Laplacian term for the type of initial conditions we use in the numerical solution. Fig. 4a shows the evolution of an initial condition at criticality. Observe that, as predicted, there is essentially no spreading. Therefore the evolution consists basically of a decay of the initial bump to 0, with an exponent that coincides with that of the bulk case: $n(t) \sim t^{-2}$. (As in the bulk case, this exponent emerges easily from the expansion of the exponential term in powers of $\int_0^\infty n(\bar{x}, s) ds$.) The area under the curves in Fig. 4a is verified to decay like t^{-2} for large times, consistent with the absence of spreading.

Supercritical Behavior. For $r > r_c$, the effective coefficient of the linear term at the origin is positive, so n grows, the initial bump spreading over all space and increasing in height until it saturates at the constant

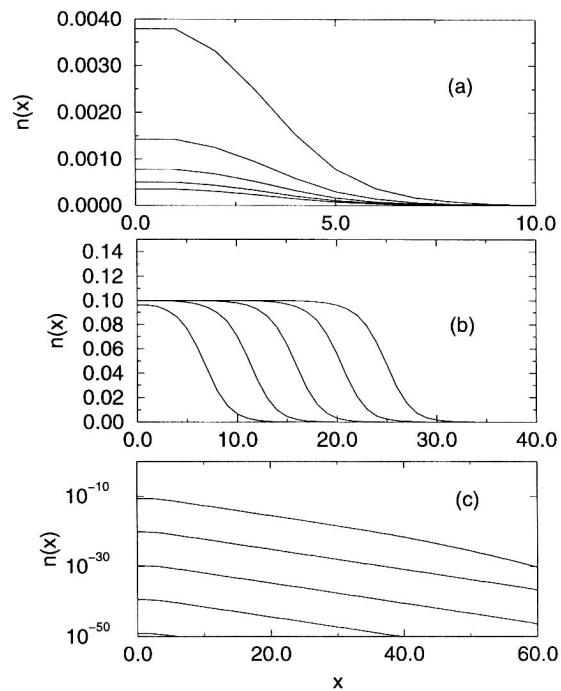


Fig. 4. Propagation of a seed in the case $\alpha = -1$, at: (a) the critical point, $r = 0.165390(2)$; (b) above the critical point ($r = 0.5$); and (c) below the critical point ($r = -0.5$). Note that the scale in (c) is semi-logarithmic. The different curves correspond to $t = 200, 400, 600, 800$ and 1000 ; $u = 5$ and $w_1 = 5$ in all cases. Note that only $x > 0$ is represented.

value r/u (see Fig. 4b). The exponential of course becomes zero asymptotically. Note that since $r_c > 0$, and since the stationary density at $r = r_c$ is zero, the density jumps discontinuously from 0 to r_c/u at $r = r_c$, giving the transition some first-order character, as in the bulk.

Subcritical Behavior. The coefficient of the effective linear term is negative, so an initial bump dies out exponentially, without spreading (see Fig. 4c).

Phase Diagram. As in the $\alpha > 0$ case, the bulk critical point separating the active and absorbing phases does not in general coincide with the one defining critical spreading of an initially localized seed. Indeed, we have seen that for $\alpha < 0$ both critical points depend on the initial condition. Typically, however, the phase diagram looks qualitatively like the one in Fig. 5. The spreading phase transition has some first-order character, as explained above. The phenomenology of the model in this case reproduces the two main features of systems in the voter model universality class: in invaded regions the density field (averaged over surviving trials) reaches a constant steady value asymptotically, and the transition separating the phase in which spreading is possible from the one in which it is not has some first-order character. We have thus far not succeeded in deriving the voter model critical exponents from (11) with $\alpha < 0$ using renormalization group arguments.

C. Higher Dimensions

Even though our numerical results are restricted to the 1D case, all the arguments presented above are essentially independent of dimension, so the

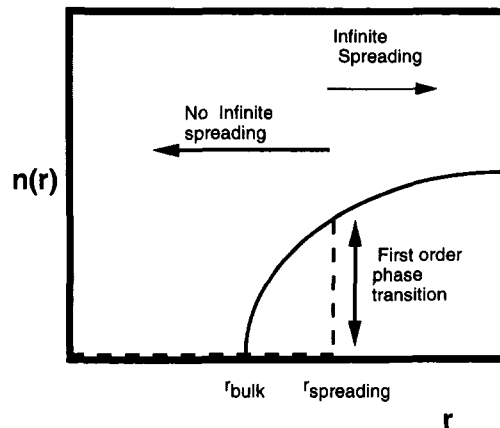


Fig. 5. Phase diagram for $\alpha = -1 < 0$; $r_{\text{spreading}} = 0.16539$.

structure of the mean-field phase diagrams should remain valid in arbitrary dimension d . It is interesting to note that, at the mean-field level, Eq. (11) gives rise to some non-universal behavior for any d . We have, for example, seen that critical exponents change with the sign of the parameter α .

IV. BEYOND THE MEAN FIELD APPROXIMATION

In the previous section we found that mean-field theory produces novel, non-trivial phase diagrams with critical points and properties that can depend on α and on the kind of initial conditions applied. We now explore whether this phase structure and non-universality persist beyond the mean-field approximation, when fluctuations are included.

Numerical simulations are the main tool we have used in this endeavor. There are two different numerical strategies one could follow. The first is to simulate Eq. (11) directly.^(43,44) The disadvantage of this route is that simulating a field theory is difficult, and obtaining asymptotic critical behavior from it is computationally expensive.⁽⁴³⁾ This strategy will thus be relegated to a separate publication.⁽⁴⁴⁾ Here we choose the second alternative, defining a discrete, microscopic model, which can be argued to belong to the universality class of Eq. (11), and which is much simpler to study numerically. The discrete model we treat is called “the non-Markovian contact process,” and is introduced in the next section.

A. The Non-Markovian Contact Process: Definition

Let us first define the standard contact process (CP) in its discrete time version.^(7,3,45) At every point, i , of a d -dimensional square lattice an occupation variable $n(i)$ which can take the values 0 or 1, is defined, $n=0$ and $n=1$ respectively describing sites that are empty and occupied by a particle. At each time step, a particle can either create a new particle on a neighboring empty site with probability p , or disappear with complementary probability $1-p$. Each newly created particle appears with equal probability at any of the nearest neighbors of the original particle. If the randomly chosen site is already occupied, the creation process is rejected. As particles cannot be generated spontaneously, it is clear that the empty lattice is an absorbing state of the model.

The non-Markovian contact process (NMCP), is a simple modification of the CP, in which p is replaced at any point i and at every discrete time step t by a history-dependent probability:

$$p(i, t) = p_0 + \alpha \exp \left[-w_1 \sum_{\tau < t} n(i, \tau) \Delta t \right] \quad (16)$$

where Δt is the discrete time increment. It is not difficult to argue that this model belongs to the universality class of Eq. (11). Using the same type of arguments employed to show that the CP is in the RFT universality class,⁽²⁵⁾ it is straightforward to conclude that the NMCP is in the universality class of a RFT-like theory with effective history-dependent parameters. Except for the mass-term, all the parameters in the ordinary RFT are marginally relevant by naive power counting at the critical dimension. Because the history-dependent corrections to these parameters are less relevant (since they involve higher powers of the field), only the history-dependent correction to the effective mass term, $r(x, t) = r_0 + \alpha \exp[-w_1 \int dt n(x, t)]$, is potentially important for critical behavior. The Langevin equation that results from these arguments is then just RFT supplemented by the non-local mass term, viz., precisely Eq. (11). This implies that the NMCP is in the same universality class as Eq. (11), and hence also in that of systems with INAS. Note that p_0 and α must be chosen to satisfy $0 < p_0 < 1$ and $0 < p_0 + \alpha < 1$, in order for $p(i, t)$ in Eq. (16) to be a true probability.

B. Numerical Procedure

In this section we report results of Monte Carlo simulations of the NMCP that start from seed initial conditions. We consider a d -dimensional lattice of variable size L^d , and implement the evolutionary rules as defined above. The algorithm is much more efficient if sites for attempted updates are chosen from a list of occupied sites.^(9,3) Sequential updating is used. As is usual in this type of simulation, with each discrete time step the time variable is incremented by $\Delta t = 1/N(t)$, where $N(t)$ is the total number of particles. The initial condition consists of an isolated particle at the origin in an otherwise empty lattice. The number of independent runs used for a given set of parameters varies, but can be as large as 10^6 . Most of the runs die for long enough times, of course. In the simulations, we measure the standard quantities, $N(t)$, $P(t)$ and $R^2(t)$, as well as the decay of the density around the origin. To compute the critical exponents associated with these quantities, we plot their logarithmic derivatives as functions of $1/t$. The intersections of these curves with $1/t = 0$ give the asymptotic values of the slopes, and therefore the critical exponents.

C. Numerical Results: One Dimension

We start with the 1D case.

1. $\alpha = 0$ Case. This corresponds to the standard CP, which is known to be in the DP universality class. As the exponents are known with

high precision, this case serves as a test of our algorithm. Using the criterion of power law behavior at criticality, we determine the critical point, and obtain $p \approx 0.7673(2)$ which is in excellent agreement with the previously known result.⁽³⁾ For the critical exponents we get $\eta \approx 0.31$, $\delta \approx 0.15$ and $z \approx 1.23$, also in very good agreement with the accepted results for DP.⁽³⁾ We also determined the bulk critical exponent θ , characterizing the decay of a homogeneous initial condition to the absorbing state at the critical point. Our best estimate was $\theta \approx 0.16$, to be compared with the known result $\theta \approx 0.159$ for DP. (Note that in the DP universality class, the exponents θ and δ are equal.)

2. $\alpha \neq 0$ Case. In this case the critical point is *not shifted* with respect to the $\alpha = 0$ case, in contrast with the mean-field predictions but in agreement with numerical results for 1D models with INAS.^(35, 40) The dynamical exponent z and the sum $\eta + \delta$ are found to be universal, taking values compatible with DP within the accuracy limits (see Table I). However, the exponents η and δ individually are not universal, depending continuously on α (see Figs. 6, 7, and 8, and Table I). Since $\alpha = \langle w_2(r_1/w_1 - n_1(\vec{x}, t=0)) \rangle$, negative values of α correspond to an excess of isolated particles with respect to the natural density in microscopic models with INAS. In this case, these microscopic models exhibit scaling with exponents $\delta > \delta_{DP}$, and $\eta < \eta_{DP}$,^(37, 39) which is precisely what we find in our simulations when $\alpha < 0$ (see Figs. 6, 7, and 8, and Table I). On the other hand, for positive α , $\delta < \delta_{DP}$ and $\eta > \eta_{DP}$, also in agreement with the results for microscopic models with INAS.

In order to verify whether the hyperscaling relation, Eq. (7), derived for systems with INAS, is satisfied,^(37, 39) we also measured θ . For all values of α we studied, the result for θ was very close to the known DP value (as expected for θ , which is a bulk exponent). Note that this implies $\theta \neq \delta$,

Table I. Numerical Values of the Critical Exponents for the 1D NMCP, for Different Values of α^a

α	η	δ	$\eta + \delta$	z	θ
-10.0	0.02	0.45	0.47	1.26	0.16
-0.5	0.24	0.22	0.46	1.27	0.155
0.0	0.31	0.16	0.47	1.27	0.16
0.15	0.33	0.14	0.47	1.27	0.155
0.5	0.36	0.11	0.47	1.26	0.16

^aThe uncertainty in all cases is ± 0.01 ; $\alpha = 0$ corresponds to DP.

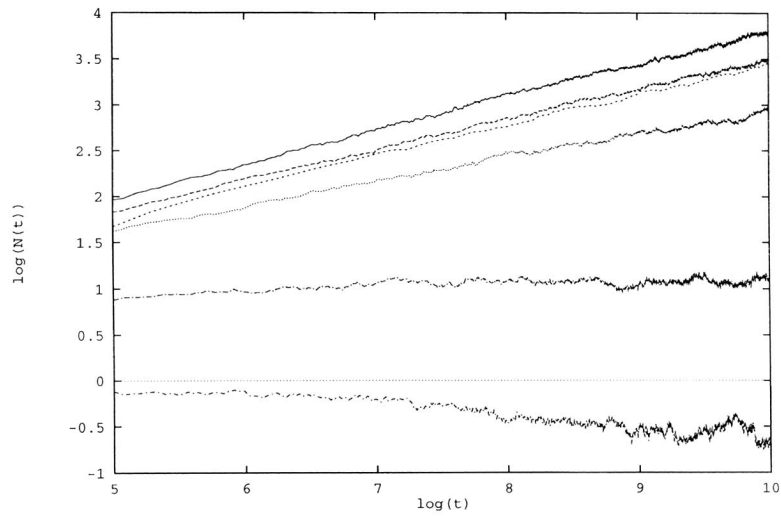


Fig. 6. Log-log plot of the time evolution of $N(t)$ at criticality, for different values of α in the 1D NMCP. From top to bottom: $\alpha = 0.5$, $\alpha = 0.15$, $\alpha = 0.0$, $\alpha = -0.5$, $\alpha = -10.0$, and $\alpha = -50.0$. The critical exponent changes continuously with α .

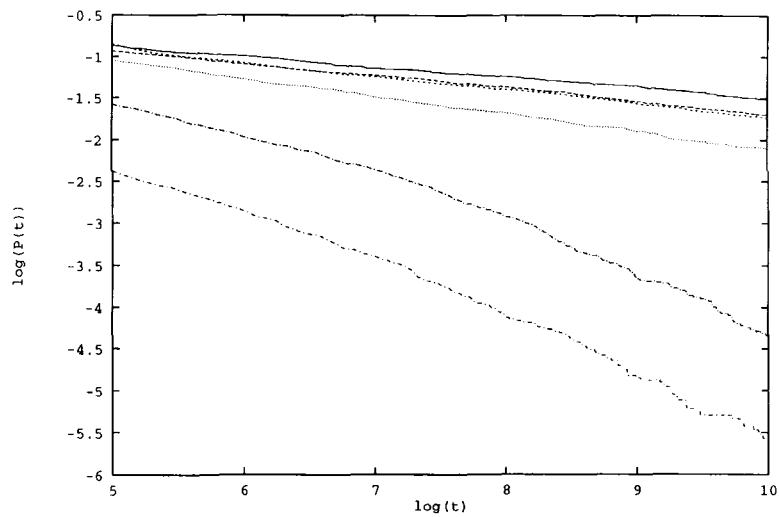


Fig. 7. Log-log plot of the time evolution of $P(t)$ at criticality, for different values of α in the 1D NMCP. From top to bottom: $\alpha = 0.5$, $\alpha = 0.15$, $\alpha = 0.0$, $\alpha = -0.5$, $\alpha = -10.0$, and $\alpha = -50.0$. The critical exponent changes continuously with α .

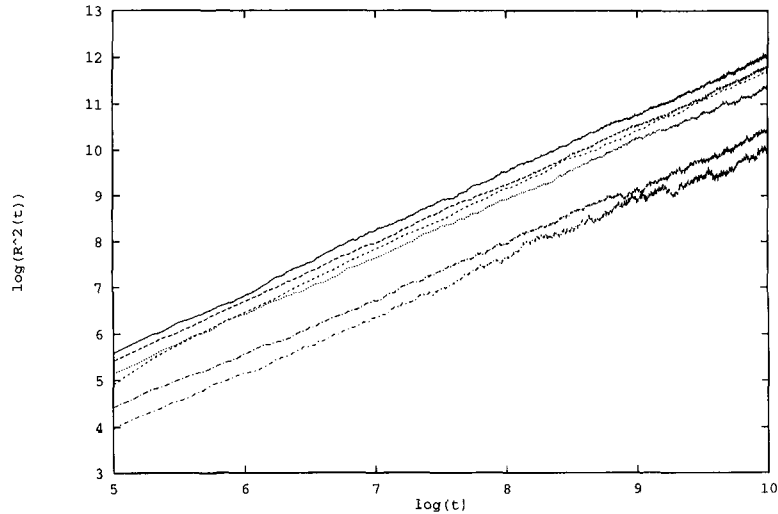


Fig. 8. Log-log plot of the time evolution of $R^2(t)$ at criticality, for different values of α in the 1D NMCP. From top to bottom: $\alpha = 0.5$, $\alpha = 0.15$, $\alpha = 0.0$, $\alpha = -0.5$, $\alpha = -10.0$, and $\alpha = -50.0$. The slope for large times is the same for all the curves.

contrary to what happens in DP. The scaling relation (7) was satisfied with good accuracy in all of our trials.

A possible explanation of the non-universality is that the measured exponent values are not the true asymptotic ones, but have yet to converge to their asymptotic DP values. To explore this possibility we ran some very large simulations (up to times $t = 250000$), with different values of the parameters α and w_1 . (Note that w_1 controls how fast the argument of the exponential term vanishes, so increasing it should make the exponential term vanish more rapidly at any occupied point, and hence promote the crossover to DP values.) Nonetheless, we found no hint of a crossover to DP exponents in any of our trials.

In summary, the Langevin Eq. (11) appears to reproduce very well all the phenomenology of microscopic 1D models with INAS. The complex phase structure observed in the mean-field approximation is destroyed by the fluctuations, and only one critical point remains. There is apparently some non-universal behavior, for which no satisfactory explanation exists at present.

D. Numerical Results: Two Dimensions

In two dimensions we expect the effect of fluctuations to be less pronounced than in $d = 1$. The mean-field phase structure is therefore more likely to be preserved.

1. $\alpha = 0$ Case. Again the case $\alpha = 0$ constitutes a good test of the algorithm. The critical point is found to be located at $p \approx 0.622$, in good agreement with the known value.⁽³⁾ The associated critical exponents are also in fairly good agreement with the expected DP values, given that we did not perform very extensive simulations to try to obtain extremely precise values. In particular, we get $\eta \approx 0.205$, $\delta \approx 0.46$, and $z \approx 1.13$, to be compared with the known results: $\eta = 0.214(2)$, $\delta = 0.460(6)$, and $z = 1.134(4)$.⁽³⁾

2. $\alpha > 0$ Case. In accord with our mean-field predictions, the critical point for spreading, $p_s(\alpha)$, is found both to be shifted downward with respect to the $\alpha = 0$ critical point, $p_s(\alpha = 0)$, and to depend on α . The critical point for bulk properties is, however, found to coincide with that of the $\alpha = 0$ case, viz., $p \approx 0.622$. We have studied in detail the case $\alpha = 0.2$, for which we get $p_s(\alpha) \approx 0.597$, using the usual criterion that the critical point be characterized by power-law behavior.

At criticality, we measure the following exponent values: $\eta \approx 0.7$, $\delta \approx 0.08$, and $z \approx 1.78$ (see Fig. 9). These values agree, to within our precision of roughly 10%, with the values for dynamical percolation in 2D, for which the best estimates we are aware of are: $\eta = 0.6$, $\delta = 0.08$ and $z = 1.76$. (See refs. 15 and 46 and also ref. 39 for the relation between the exponents defined and measured in ref. 15 and the ones we study here.) In Fig. 10 we show the evolution of the averaged particle density $\langle n(x, y = 0) \rangle$ as a function of the distance x to the initial seed. A similar structure to that predicted in mean field is observed, namely, the initial bump splits into two pieces, which separate from each other in time. (In fact, of course, there is an expanding ring, which leaves behind it an empty circular region. Only a 1D cut of this ring is shown in the figure.) At the bulk critical point, we measure $\theta \approx 0.46$ which coincides with the DP value. Therefore, we have fairly clear evidence that the dynamical percolation behavior for spreading predicted by mean-field theory survives fluctuations, that the bulk properties are DP-like, and the mean field phase structure (Fig. 3) is qualitatively valid.

3. $\alpha < 0$ Case. The critical point for bulk properties is at $p \approx 0.622$, and, as in the previous cases, $\theta \approx 0.46$, indicating that these properties are DP-like, and do not depend on α .

The critical value, $p_s(\alpha)$, for spreading seems to be very slightly larger than $p_s(0)$. In particular, for $\alpha = -0.1$ we get $p_s(\alpha) \approx 0.625$. The critical exponents η , δ , $\eta + \delta$, and z (Fig. 11) all appear to vary continuously with the parameters of the model, such as α and w_1 . This is consistent with the behavior reported in ref. 40, and represents even more severe nonuniversality than occurs in 1D, where z and $\eta + \delta$ assume universal, DP values.

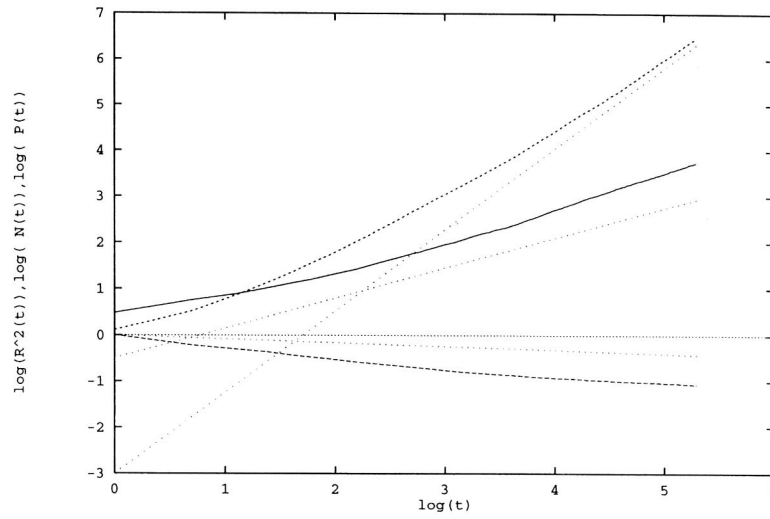


Fig. 9. Log-log plots of (from top to bottom) $R^2(t)$, $N(t)$, and $P(t)$ for the 2D NMCP, at the critical point, for $\alpha = 0.2$. The dotted lines correspond to the asymptotic behaviors for the dynamical percolation universality class.

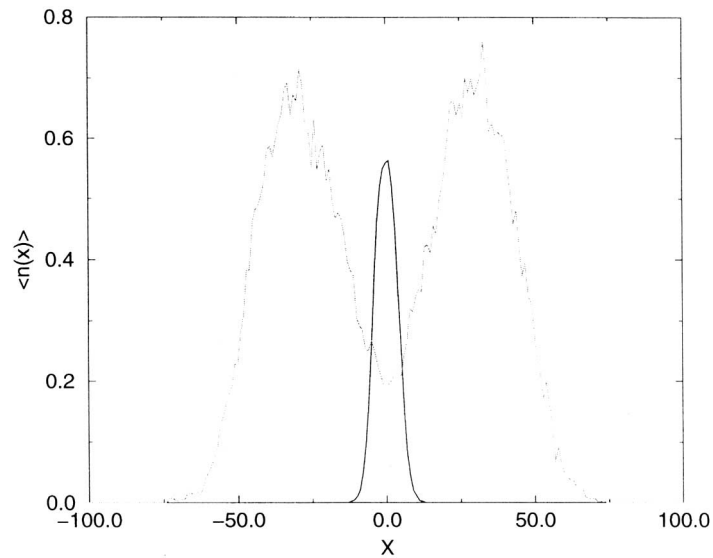


Fig. 10. The averaged particle density $\langle n(x, y = 0) \rangle$ averaged over 10000 runs, in the case $\alpha > 0$, at the critical point of the 2D NMCP. The initial condition (solid line), and the profile at $t = 300$ (dotted line), are represented. The initial bump splits in two with increasing time.

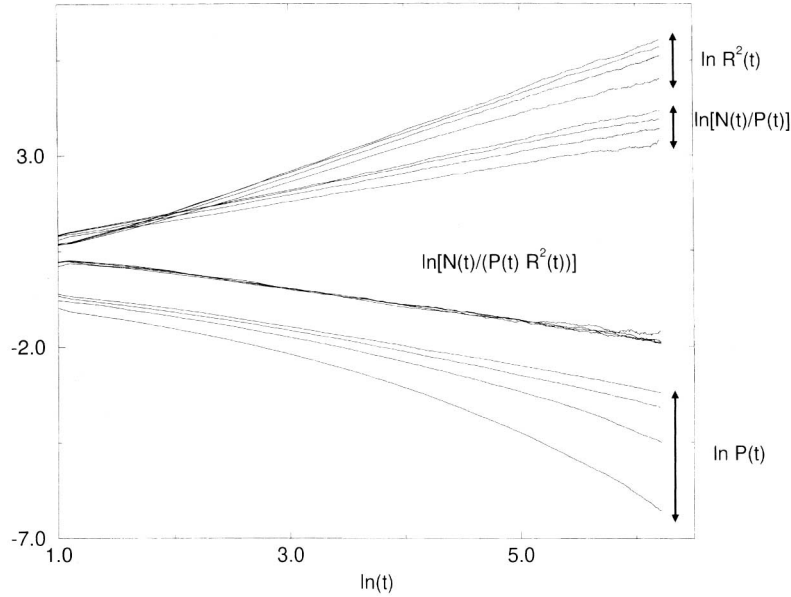


Fig. 11. Log-log plots of (from top to bottom) $R^2(t)$, $N(t)/P(t)$, $N(t)/P(t) R^2(t)$, and $P(t)$, respectively corresponding to the exponents z , $\eta + \delta$, $\eta + \delta - z$, and $-\delta$, at the critical point of the 2D NMCP. The four curves in the data set for each quantity correspond to, from top to bottom: $(w_1, \alpha) = (100.0, -0.1)$, $(1.0, -0.05)$, $(1.0, -0.1)$, $(1.0, -0.2)$.

Figure 11 shows, however, that the combination $\eta + \delta - z$ remains universal, consistent with the scaling relation^(37, 35, 39)

$$\eta + \delta - dz/2 = -\theta \tag{17}$$

where the bulk exponent θ assumes its DP value⁽⁴²⁾ of roughly 0.46. Note that the data of ref. 40 apparently do not obey this scaling law. Since the scaling law seems rather fundamental (e.g., ref. 39), we are inclined to attribute this to the difficulties of achieving the asymptotic limit for critical behavior in 2D simulations. Figure 11 makes clear, for example, that our log-log data for the survival probability governing the exponent δ are quite curved, implying that the asymptotic limit has not yet been reached. The data for $\eta + \delta - z$, by contrast, are very linear. It is of course possible that the observed nonuniversality and the apparent difficulties in reaching the asymptotic regime are connected with the proximity of the CDP fixed point discussed in section III in the context of mean-field theory. Clearly more extensive simulations will be required to resolve these difficult issues.

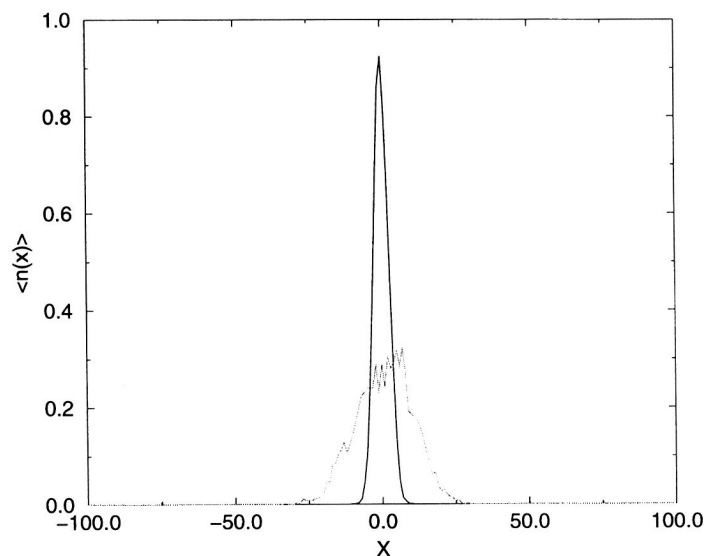


Fig. 12. One-dimensional cut of the particle density at $\alpha = -0.1$, averaged over 10000 runs, in the case $\alpha < 0$ at the critical point of the 2D NMCP. The initial condition (solid), and the profile at $t = 300$ (dotted), are represented.

In Fig. 12 we show the particle density, $\langle n(x, y=0) \rangle$, for $\alpha = -0.1$, averaged over *all* trials, as a function of the distance x to the origin, for two different times. There is a very slow spreading, and the integral over the curves decreases slowly in time, corresponding to $\eta \sim -0.1$.

4. Two-Dimensional Systems With INAS Revisited. With the results of the mean-field analysis and the numerics in mind, we now reassess the conclusions drawn in ref. 40, where critical spreading in two dimensions for systems with INAS was first studied numerically. We propose that the apparent non-universality observed in ref. 40 is in fact a consequence of the 2D NMCP having three different possible critical behaviors, corresponding to DP, dynamical percolation, and the non-universal regime discussed in the previous subsection. Which one of these is observed in any given case depends on the quantity measured and on the parameter values. In particular, for the case of an initial density smaller than the natural one (e.g., $\phi = 0.2$ in the notation of ref. 40, corresponding to $\alpha > 0$ in ours), there is a shift in the critical point for spreading consistent with the one predicted by mean-field theory and observed to occur in the 2D NMCP with $\alpha > 0$. The spreading exponents measured in ref. 40 for

this case are $\eta = 0.64$, $\delta = 0.078$, and $z = 1.84$, in reasonably good agreement with the 2D dynamical percolation values, (0.60, 0.08, and 1.76, respectively), suggested by our analysis. The qualitative picture of an expanding ring of activity described in ref. 40 is also consistent with the phase transition being in the dynamical percolation universality class. The bulk exponents measured in that reference are DP-like, as expected from our analysis and the field theoretical arguments presented in ref. 36.

On the other hand, in the case where the density of the initial absorbing environment exceeds the natural value (e.g., $\phi = 0.5$ in the notation of ref. 40, corresponding to $\alpha < 0$), the observed nonuniversality is qualitatively consistent with our measurements on the NMCP. The main difference is that the scaling law $\eta + \delta - dz/2 = -\theta$, satisfied by the NMCP, is apparently violated in ref. 40. We attribute this to the fact that, as noted in ref. 40, the measured values of the exponents in that work are not the true asymptotic ones.

V. CONCLUSIONS

We now summarize the implications of our analytic and numerical results on the non-Markovian contact process and systems with infinite numbers of absorbing states:

- In both one and two dimensions, the critical properties of bulk quantities measured in simulations with spatially homogeneous initial conditions are universal, and belong in the directed percolation universality class, as predicted in ref. 36.

- In two dimensions, the phase structure for spreading properties depends importantly on the sign of α . For $\alpha > 0$, critical spreading in the NMCP occurs at a value of the parameter p smaller than the bulk critical value, and critical spreading exponents fall in the dynamical percolation universality class. For $\alpha < 0$, the critical value of p for spreading seems to be very slightly above the bulk critical value. Spreading exponents are apparently nonuniversal, but the scaling law $\eta + \delta - dz/2 = -\theta$ is satisfied, with θ assuming its universal, DP value.

- In one dimension, there is a unique critical point at which both bulk and spreading behaviors become singular. All critical spreading properties associated with quantities averaged only over surviving runs are universal and DP-like, but those defined by averaging over all runs, and hence involving the survival probability, appear to be nonuniversal. Unlike in the 2D case, the exponents z and $\eta + \delta$ assume universal DP values in 1D.

- The nonuniversality observed in both 1D and 2D for $\alpha < 0$ is not predicted by mean-field theory, indicating that fluctuation effects are rather severe. As yet there is no satisfactory explanation for this nonuniversality in either field theoretical arguments or series expansions.

ACKNOWLEDGMENTS

This work was partially supported by the European Union, through a grant to M.A.M. We acknowledge useful discussions with Pedro L. Garrido, Cristóbal López and Yuhai Tu.

NOTE ADDED IN PROOF

After completing this work, we became aware of a paper by P. Grassberger, H. Chaté, and H. Rosseau [*Phys. Rev. E* **55**, 2488 (1997)]—GCR hereafter—where the similar problem of spreading in media with long-time memory is studied. Some of the conclusions in that paper correspond to ours here. The main differences are, firstly, that GCR argue rather convincingly that the critical point for spreading in what amounts to our $\alpha < 0$ case is identical to the bulk critical point. Our 2D data, which show only a very slight shift in p_c with α , are compatible with this conclusion. Secondly, GCR's numerical data in 2D do not satisfy the scaling law $\eta + \delta - dz/2 = -\theta$, presumably because they have not achieved the asymptotic limit. Indeed, they show considerable curvature.

REFERENCES

1. S. R. Broadbent and J. M. Hammersley, *Proc. Camb. Philos. Soc.* **53**:629 (1957).
2. *Percolation Structures and Processes*, G. Deutscher, R. Zallen, and J. Adler, eds., Annals of the Israel Physical Society, Vol. 5 (Hilger, Bristol, 1983).
3. J. Marro and R. Dickman, *Nonequilibrium Phase Transitions and Critical Phenomena* (Cambridge University Press, Cambridge, 1996).
4. J. Kohler and D. ben-Avraham, *J. Phys. A* **24**:L621 (1991); D. ben-Avraham and J. Kohler, *J. Stat. Phys.* **65**:839 (1992).
5. E. V. Albano, *J. Phys. A* **25**:2557 (1992); A. Maltz and E. V. Albano, *Surf. Sci.* **277**:414 (1992).
6. H. Takayasu and A. Yu. Tretyakov, *Phys. Rev. Lett.* **68**:3060 (1992); I. Jensen, *Phys. Rev. E* **50**:3623 (1994).
7. T. E. Harris, *Ann. Phys.* **2**:969 (1974).
8. I. Jensen, H. C. Fogedby and R. Dickman, *Phys. Rev. A* **47**:3411 (1990).
9. R. M. Ziff, E. Gulari, and Y. Barshad, *Phys. Rev. Lett.* **56**:2553 (1986).
10. A. S. Pikovsky and J. Kurths, *Phys. Rev. E* **49**:898 (1994).
11. G. Grinstein, M. A. Muñoz, and Y. Tu, *Phys. Rev. Lett.* **76**:4376 (1996); Y. Tu, G. Grinstein, and M. A. Muñoz, *Phys. Rev. Lett.* **78**:274 (1997).

12. M. A. Muñoz and T. Hwa, *Europhys. Lett.* **41**:147 (1998).
13. M. J. Howard and U. Tauber, Preprint, cond-mat/9701069.
14. P. Grassberger, *J. Stat. Phys.* **79**:13 (1995).
15. P. Grassberger, *Math. Biosci.* **63**:157 (1983).
16. J. Cardy, *J. Phys. A* **16**:L709 (1983).
17. J. L. Cardy and P. Grassberger, *J. Phys. A* **18**:L267 (1985); H. K. Janssen, *Z. Phys. B* **58**:311 (1985).
18. K. De'Bell and J. W. Essam, *J. Phys. A* **16**:3145 (1986).
19. See, for instance, A. L. Barabasi, G. Grinstein, and M. A. Muñoz, *Phys. Rev. Lett.* **76**:1481 (1996), and references therein.
20. M. Paczuski, S. Maslov, and P. Bak, *Europhys. Lett.* **27**:97 (1994); R. Dickman, A. Vespignani, and S. Zapperi, *Phys. Rev. E* **57**:5095 (1998).
21. P. Grassberger and A. de la Torre, *Ann. Phys. (N.Y.)* **122**:373 (1979).
22. H. K. Janssen, *Z. Phys. B* **42**:151 (1981).
23. P. Grassberger, *Z. Phys. B* **47**:365 (1982).
24. H. D. I. Abarbanel and J. B. Bronzan, *Phys. Rev. D* **9**:2397 (1974).
25. J. L. Cardy and R. L. Sugar, *J. Phys. A* **13**:L423 (1980); H. K. Janssen, *Z. Phys. B* **42**:151 (1981).
26. See, for instance, I. Jensen, *Phys. Rev. A* **45**:R563 (1992), and references therein.
27. G. Grinstein, Z.-W. Lai, and D. A. Browne, *Phys. Rev. A* **40**:4820 (1989).
28. E. Domany and W. Kinzel, *Phys. Rev. Lett.* **53**:311 (1984); J. W. Essam, *J. Phys. A* **22**:4927 (1989).
29. L. Peliti, *J. Phys. A* **19**:L365 (1986).
30. R. Dickman and A. Yu. Tretyakov, *Phys. Rev. E* **52**:3218 (1995).
31. P. Grassberger, F. Krause, and T. von der Twer, *J. Phys. A* **17**:L105 (1984); P. Grassberger, *J. Phys. A* **22**:L1103 (1989); M. H. Kim and H. Park, *Phys. Rev. Lett.* **73**:2579 (1994); N. Menyhard, *J. Phys. A* **27**:6139 (1994).
32. J. Cardy and U. C. Täuber, *Phys. Rev. Lett.* **77**:4780 (1996).
33. D. A. Browne and P. Kleban, *Phys. Rev. A* **40**:1615 (1989).
34. K. Yaldram, K. M. Khan, N. Ahmed, and M. A. Khan, *J. Phys. A* **26**:L801 (1993).
35. I. Jensen and R. Dickman, *Phys. Rev. E* **48**:1710 (1993); I. Jensen, *Int. J. Mod. Phys. B* **8**:3299 (1994); I. Jensen, *Phys. Rev. Lett.* **70**:1465 (1993).
36. M. A. Muñoz, G. Grinstein, R. Dickman, and R. Livi, *Phys. Rev. Lett.* **76**:451 (1996).
37. J. F. F. Mendes, R. Dickman, M. Henkel, and M. C. Marques, *J. Phys. A* **27**:3019 (1994).
38. T. E. Harris, *Ann. Prob.* **2**:969 (1974).
39. M. A. Muñoz, G. Grinstein, and Y. Tu, Survival Probability and Field Theory in Systems with Absorbing States, *Phys. Rev. E* **56**:5101 (1997).
40. R. Dickman, *Phys. Rev. E* **53**:2223 (1996).
41. G. Grinstein and A. Luther, *Phys. Rev. B* **13**:1329 (1976).
42. M. A. Muñoz, G. Grinstein, R. Dickman, and R. Livi, *Physica D* **103**:485 (1997).
43. A numerical scheme to analyze Langevin equations with absorbing states was proposed recently: R. Dickman, *Phys. Rev. E* **50**:4404 (1994); see also ref. 44, for the application of that technique to the Langevin equation discussed in this work.
44. C. López and M. A. Muñoz, Numerical analysis of a Langevin equation for systems with infinite absorbing states, *Phys. Rev. E* **56**:4864 (1997).
45. T. M. Liggett, *Interacting Particle Systems* (Springer-Verlag, New York, 1985).
46. Z. Alexandrovich, *Phys. Lett. A* **80**:284 (1980).